TECHNIQUES

by M. Ragulskis, R. Maskeliunas, and L. Ragulskis

PLOTTING MOIRÉ FRINGES FOR CIRCULAR STRUCTURES FROM FEM RESULTS

Procedures for plotting computer generated moiré mechanical interference bands (moiré fringes) from the results of finite element analysis can provide meaningful information about the processes taking place in the analysed structures. Such visualization is important from the point of view of interpretation of experimental results[2,7] and enables calculation of structural stresses with sufficient accuracy.[1,8] Computer generated moiré fringes produced from the overlap of two repetitive patterns can give a realistic view of the structural deformations. Moreover, the digital plotting procedures of moiré fringes can also be effectively applied for the visualization of periodic dynamic processes if the structure is stroboscopically photographed in the states of equilibrium and the states of extreme displacements.

Numerical generation of realistic fringe patterns requires non-trivial computer code implementations. The sufficient smoothness of the interfering grids must be considered. That requires the utilisation of multiple intensity levels and incorporation of 3D graphical models. On the other side, the discrete FEM results must be interpolated over the domain of the structure. Visualisation of small deformations around the state of equilibrium without exaggerating the nodal displacements also requires appropriate adaptations.

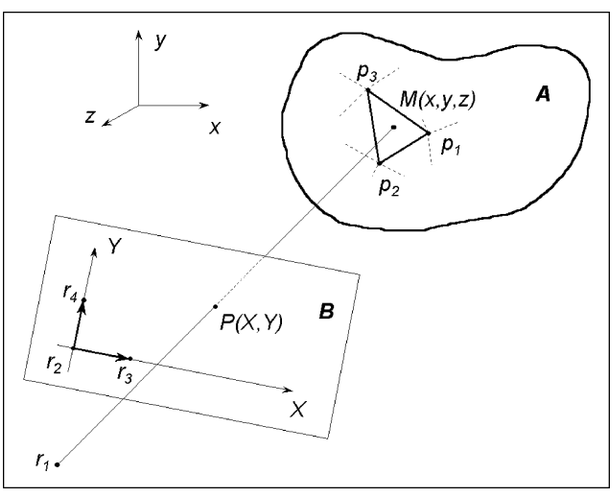

Fig. 1: Construction of the digital image

The commonly used repetitive patterns for the generation of moiré fringes are interference grids formed from arrays of parallel straight lines. Application of such grids for the structures of circular type faces quite severe complications due to the interpretation of angular and radial displacements. Moreover, application of straight parallel grid lines in some experimental set-ups involving dynamic analysis of circular structures is practically impossible.

Therefore the numerical procedures generating realistic moiré fringe patterns for different structural geometries are important and useful tools for visualization of numerical analysis data and interpretation of experimental results.

M. Ragulskis (SEM Member) is an Associate Professor at Kaunas University of Technology, Lithuania. R. Maskeliunas (SEM Member) is Research Fellow at Vilnius Gediminas Technical University, Lithuania. L. Ragulskis is Research Associate at Vytautas Magnus University, Lithuania.

CONSTRUCTION OF THE DIGITAL IMAGE

Let the coordinates of the point r_1 define the observation point and the projection plane be defined by the points r_2, r_3 and r_4 and vectors $(r_3 - r_2)$, $(r_4 - r_2)$ form the ortho-normal base of the projection plane (Fig. 1):

$$r_i = (x_i, y_i, z_i), \quad i = 1,2,3,4. \tag{1}$$

Let the planar structure in the state of plane stress be meshed by the finite element method and be located in the plane '*A*' which coincides with the plane $z = 0$. It is assumed that the analysed structure performs in-plane vibrations.

The location of every point $M\ (x, y, z)$ on the surface of the structure can be expressed through the shape functions of the appropriate finite element.[1] Three shape functions L_1, L_2 and L_3 are associated to a finite element $\{p_1, p_2, p_3\}$ if the triangular elements are used for meshing (Fig. 1).

Similarly, the location of the point of intersection $P(\tilde{x}, \tilde{y}, \tilde{z})$ between the line r_1M and the projection plane B can be expressed through the parameters L_4 and L_5 (L-coordinates of the point P):

$$\begin{aligned} \tilde{x} &= L_4 x_1 + L_5 x \\ \tilde{y} &= L_4 y_1 + L_5 y \\ \tilde{z} &= L_4 z_1 + L_5 z \end{aligned} \tag{2}$$

$$L_4 + L_5 = 1$$

The numerical values of those L-coordinates can be obtained from the solution of the following system of linear algebraic equations

$$\begin{bmatrix} x_2 & x_3 & x_4 & -x_1 & -x \\ y_2 & y_3 & y_4 & -y_1 & -y \\ z_2 & z_3 & z_4 & -z_1 & -z \\ 1 & 1 & 1 & 0 & 0 \\ 0 & 0 & 0 & 1 & 1 \end{bmatrix} \begin{Bmatrix} L_1 \\ L_2 \\ L_3 \\ L_4 \\ L_5 \end{Bmatrix} = \begin{Bmatrix} 0 \\ 0 \\ 0 \\ 1 \\ 1 \end{Bmatrix} \tag{3}$$

Plotting of intensity levels in the projection plane requires the calculation of the coordinates of the point P in the projection plane. Those coordinates can be calculated as the projections of the vector $(P - r_2)$ to the appropriate axes of the projection plane:

$$\begin{aligned} X = (\tilde{x} - x_2)(x_3 - x_2) + (\tilde{y} - y_2)(y_3 - y_2) \\ + (\tilde{z} - z_2)(z_3 - z_2) \end{aligned} \tag{4}$$

PLOTTING MOIRÉ FRINGES FROM FEM RESULTS

$$Y = (\tilde{x} - x_2)(x_4 - x_2) + (\tilde{y} - y_2)(y_4 - y_2) + (\tilde{z} - z_2)(z_4 - z_2)$$

Nevertheless, such straightforward definition of the coordinates of the point in the projection plane is not efficient from the point of view of computational resources. If the projection plane is interpreted as a matrix of pixels, then the inverse problem is much more effective. Namely, if the coordinates of the observation point and a pixel in the projection plane are specified, then the appropriate point on the surface of the structure can be found as described below. Moreover, the resulting values describing the location of the point M are not its coordinates in the space xyz, but its L–coordinates. Such representation is extremely useful when the calculations are coupled with the data from FEM—all the information about the analysed structure is concentrated in discrete nodes of the FEM mesh.

The calculation of the intensity level at an appropriate pixel in the projection plane is assumed to be dependent on the in-plane displacements at point M. The definition of point M by its L–coordinates is advantageous due to the simplicity of reconstruction of the displacements at point M from the nodal displacements of the appropriate finite element. L_1, L_2 and L_3 are in fact the shape functions of the finite element.

The solution of the inverse problem involves the following calculations. The unit normal vector of the projection plane denoted by (x_0, y_0, z_0) is determined as the vector product of $(r_3 - r_2)$ and $(r_4 - r_2)$. The spatial coordinates of $P(\tilde{x}, \tilde{y}, \tilde{z})$ can be found from the following system of equations:

$$\begin{bmatrix} x_3 - x_2 & y_3 - y_2 & z_3 - z_2 \\ x_4 - x_2 & y_4 - y_2 & z_4 - z_2 \\ x_0 & y_0 & z_0 \end{bmatrix} \begin{Bmatrix} \tilde{x} \\ \tilde{y} \\ \tilde{z} \end{Bmatrix} = \begin{Bmatrix} X + x_2(x_3 - x_2) + y_2(y_3 - y_2) + z_2(z_3 - z_2) \\ Y + x_2(x_4 - x_2) + y_2(y_4 - y_2) + z_2(z_4 - z_2) \\ x_2x_0 + y_2y_0 + z_2z_0 \end{Bmatrix} \quad (5)$$

The third equation from the system (5) expresses the orthogonality of the vector $(P - r_2)$ to the normal vector of the projection plane.

As the analysed structure is located in the plane $z = 0$, and $(\hat{x}_i, \hat{y}_i)$, $i = 1,2,3$ denote the nodal coordinates of a linear triangular element, the L-coordinates of the point M can be determined from:

$$\begin{bmatrix} \hat{x}_1 & \hat{x}_2 & \hat{x}_2 & -x_1 & -\tilde{x} \\ \hat{y}_1 & \hat{y}_2 & \hat{y}_2 & -y_1 & -\tilde{y} \\ 0 & 0 & 0 & -z_1 & -\tilde{z} \\ 1 & 1 & 1 & 0 & 0 \\ 0 & 0 & 0 & 1 & 1 \end{bmatrix} \begin{Bmatrix} L_1 \\ L_2 \\ L_3 \\ L_4 \\ L_5 \end{Bmatrix} = \begin{Bmatrix} 0 \\ 0 \\ 0 \\ 1 \\ 1 \end{Bmatrix} \quad (6)$$

The line intersects the plane A inside the analysed finite triangular element when the conditions $L_i \in [0,1]$, $i = 1,2,3$ are satisfied. The L-coordinates when referred to a triangle as a finite element represent its shape functions (in our case L_1, L_2 and L_3). Here those functions are used in a more general context exploiting the advantage of the straightforward determination of the location of the intersection point with respect to the appropriate triangle. Thus the approximate coordinates of the point $M(\alpha, \beta, 0)$ are obtained by interpolation using the calculated L–coordinates.

The presented methodology can be generalised for higher order elements which can be subdivided into triangles. The approximate local coordinates of the element can be obtained by interpolation from the local coordinates of the nodes of the triangle. This is applicable for higher order elements with small deformations of their geometry. More complicated cases require the calculation of the intersection between the surface of the structure and the line using the general methods of three dimensional computer graphics.

CONSTRUCTION OF MOIRÉ FRINGE PATTERNS

It is assumed that FEM analysis is based on the linear theory of elasticity. Therefore, if the nodal deformations (or amplitudes of harmonic oscillation used for stroboscopic analysis) in the direction of the x and y axes are defined as u and v it is possible to find the original locations of points in the state of equilibrium, when their positions in the deformed structure are defined. If the coordinates of a point on the deformed surface are (α, β), then this point in the state of equilibrium had the coordinates $(\alpha - u, \beta - v)$. This reconstruction can be performed for any interpolated point on the analysed surface. Such methodology enables the preservation of the optical shape of the structure and eliminates the need for exaggerating small deformations around the status of equilibrium.

In order to obtain better interpretable moiré fringes the smooth variation of the intensity of the fringes on the surface of the object is proposed. It is assumed that the intensity varies according to the harmonic law. The intensities of lines on the object in the state of equilibrium correspond to the first term in the following expressions, the other term corresponds to the deformed status of the structure:

$$I = \cos^2\left(\frac{2\pi\alpha}{\lambda}\right) + \cos^2\left(\frac{2\pi(\alpha - u)}{\lambda}\right) \quad (7)$$

$$I = \cos^2\left(\frac{2\pi\beta}{\lambda}\right) + \cos^2\left(\frac{2\pi(\beta - v)}{\lambda}\right) \quad (8)$$

where λ is the constant defining the distance between the grid lines, I stands for intensity level, Eq. (7) represents the isothethes of u, Eq. (8) represents the isothethes of v.

The concept of isothethes is used in the description of moiré fringes in [1] and concerns the image obtained by the overlapping of the image of the lines on the structure in equilibrium and in the deformed status.

Two maps must be built separately for identifying moiré fringes in appropriate directions. The direction of the parallel grid lines can be varied by elementary rotations of the structure.

PLOTTING MOIRÉ FRINGES FROM FEM RESULTS

It can be noted, that the interpretation of moiré isothethes is not trivial. Fig. 2 shows the geometry of the structure in equilibrium (grey lines) and the third eigenmode (dark solid lines) of a rectangular plate with fastened lower edge. It is assumed that the displacements in both directions on the lower edge of the plate in the state of plain stress are equal to zero, elsewhere the structure is free. The external excitation is not stated explicitly and is assumed to be harmonic with the resonant frequency of this eigenmode and is not orthogonal to it. Thus it is possible to excite only this mode (assuming it is not multiple) with negligible contribution of the other modes, and to analyse its steady state motion by using stroboscopic photography. The nodal displacements are exaggerated with respect to the dimensions of the structure, the mesh is quite coarse. The constructed moiré fringe patterns in two planar directions are presented in Fig. 3 and Fig. 4. Isolines of displacements in both directions are constructed to validate the formation of isothethes (Fig. 5 and Fig. 6). Isolines represent the lines on the surface of the structure on which the analysed quantity takes constant values. The density of isolines indicates the rapidity of change of the represented quantity. The presented methodology enables generation of smooth moiré patterns from a relatively rough FEM approximation.

MOIRÉ FRINGES FOR CIRCULAR STRUCTURES

Application of arrays of straight lines for circular structures can lead to certain complications. Circular structures are such structures the experimental analysis of which is more convenient to perform by using the polar system of coordinates. For example, the use of parallel lines for investigation of deformations of a rotating element of a printing machine would give no practical results (Fig. 7). Modified moiré patterns can be used for circular or ring type structures enabling identification of angular and radial deformations.

The modified polar moiré patterns enable determination of the intensity for the isothethes of the polar angle. It can be calculated on the basis of the following relationship:

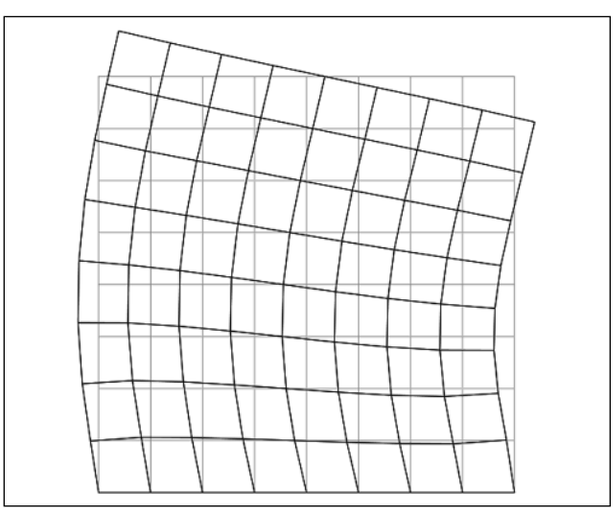

Fig. 2: The geometry and the third eigenmode of the plate

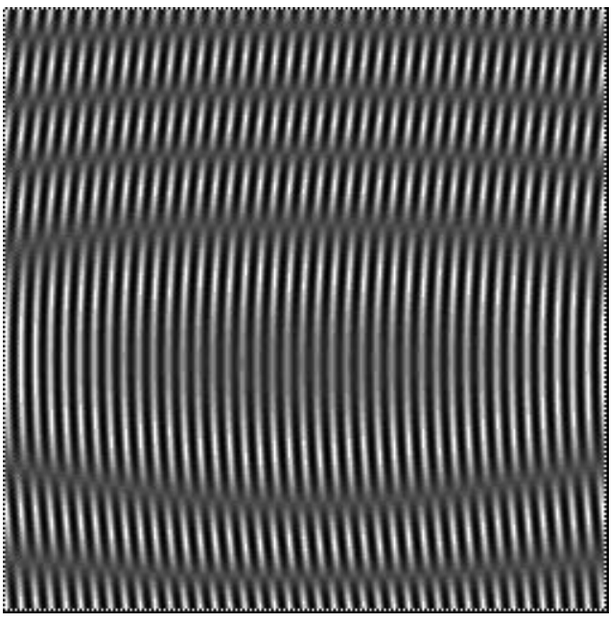

Fig. 3: Generated moiré fringes for the displacement in the direction of the *x* axis

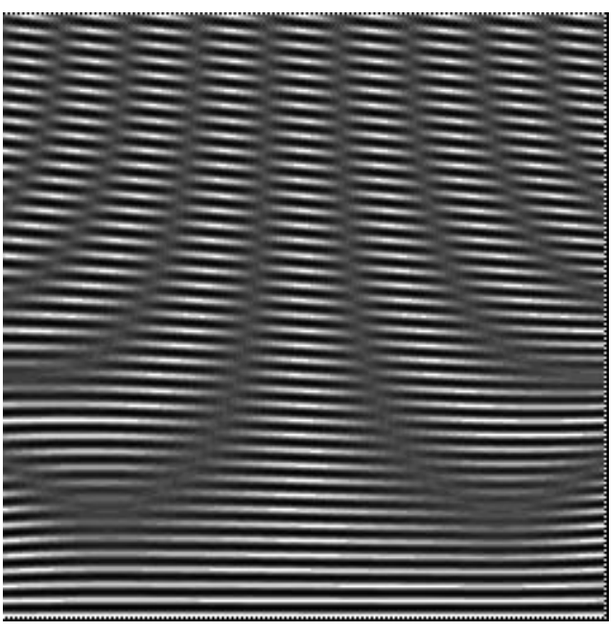

Fig. 4: Generated moiré fringes for the displacement in the direction of the *y* axis

$$I = \cos^2\left(k \cdot \operatorname{arctg}\frac{\beta}{\alpha}\right) + \cos^2\left(k \cdot \operatorname{arctg}\frac{\beta - v}{\alpha - u}\right) \quad (9)$$

where k is the constant determining the number of the radial lines. It can be noted that the thickness of the radial lines increases with the radius.

PLOTTING MOIRÉ FRINGES FROM FEM RESULTS

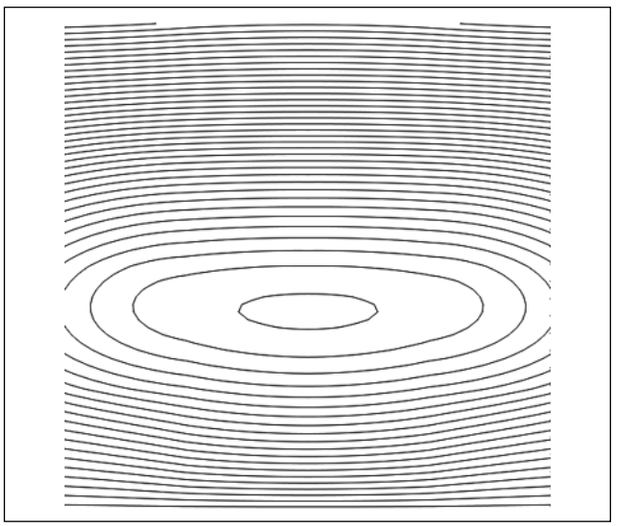

Fig. 5: The isolines of the displacement in the direction of the *x* axis

Analogously, the intensity for the isothethes of the radius can be calculated from:

$$I = \cos^2\left(\frac{2\pi}{\lambda}\sqrt{\alpha^2+\beta^2}\right) + \cos^2\left(\frac{2\pi}{\lambda}\sqrt{(\alpha-u)^2+(\beta-v)^2}\right) \quad (10)$$

where λ determines the distance between the concentric lines.

Fig. 8 shows the geometry of the structure in the state of equilibrium (grey lines) and the tenth eigenmode of a ring type structure (dark lines) with fastened internal radius (the displacements in both directions on the internal radius are assumed to be equal to zero, elsewhere the structure is free). The excitation is not stated explicitly because of the same reasons as in the previous plate analysis problem. Due to the curvilinear character of the moiré lines the moiré patterns reproduce not the isolines of displacements, but the isolines of the change of the angle (Fig. 9):

$$\operatorname{arctg}\left(\frac{\beta-v}{\alpha-u}\right) - \operatorname{arctg}\left(\frac{\beta}{\alpha}\right) \quad (11)$$

and of the change of the radius (Fig. 10):

$$\sqrt{(\alpha-u)^2+(\beta-v)^2} - \sqrt{\alpha^2+\beta^2} \quad (12)$$

The validation of moiré patterns is presented in Fig. 11 and Fig. 12. The moiré fringe patterns are difficult to comprehend, so the construction of the isolines helps for their better validation and interpretation.

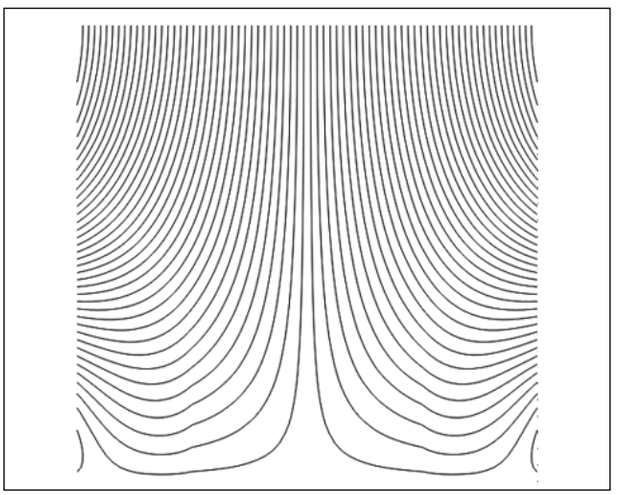

Fig. 6: The isolines of the displacement in the direction of the *y* axis

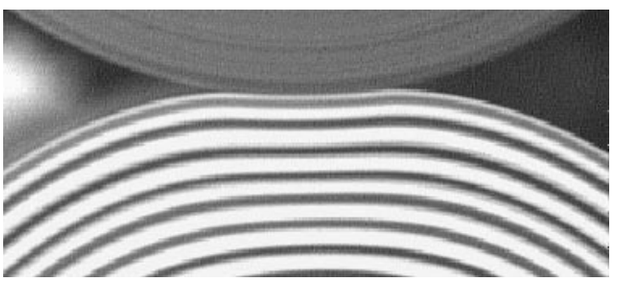

Fig. 7: Experimental investigation of a rotating contact cylinder in a printing machine

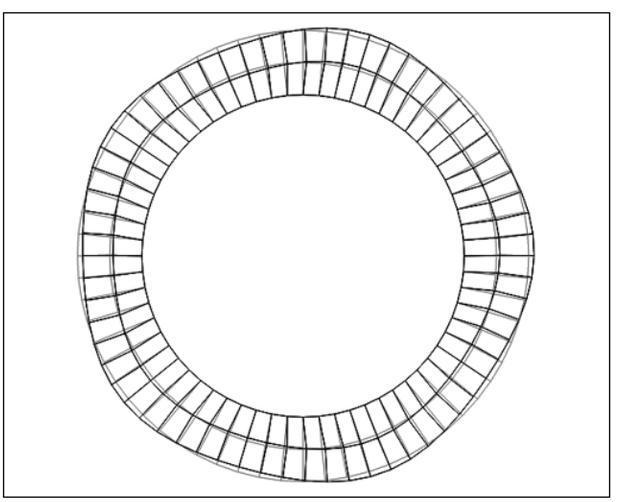

Fig. 8: The geometry and the tenth eigenmode of the ring-type structure

PLOTTING MOIRÉ FRINGES FROM FEM RESULTS

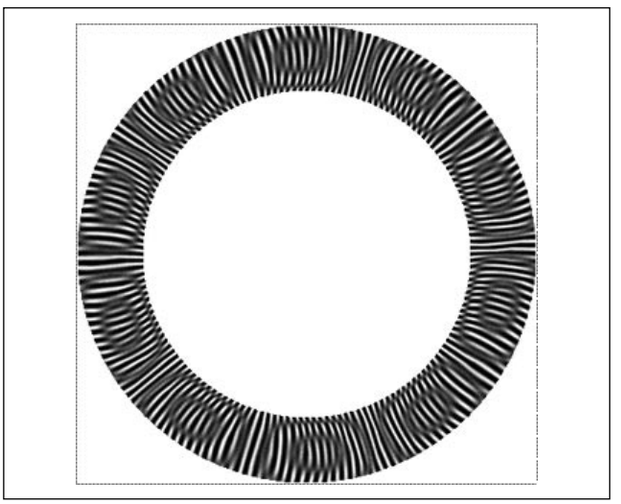

Fig. 9: Generated moiré fringes for the angular displacement

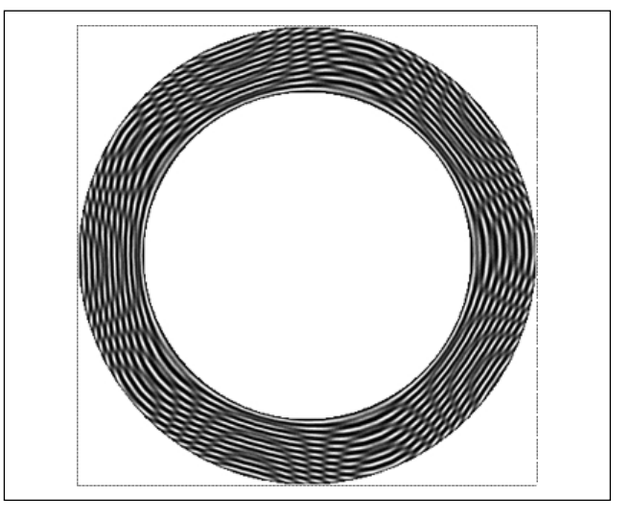

Fig. 10: Generated moiré fringes for the radial displacement

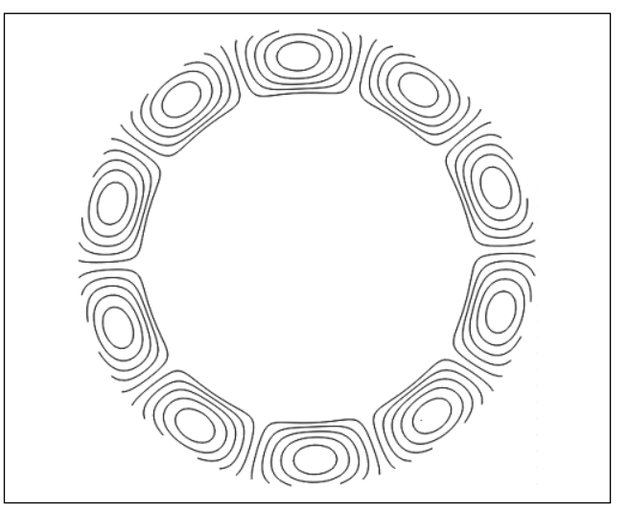

Fig. 11: The isolines of the variation of the angle

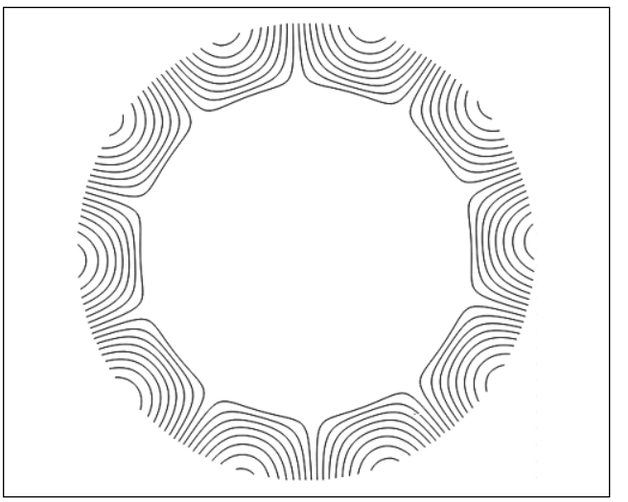

Fig. 12: The isolines of the variation of the radius

CONCLUSIONS

Plotting of moiré fringes from the results of finite element calculations is important because of the ability of direct comparisons with the experimental results of analysis. The smooth variation of the intensity of the lines on the surface of the structure according to the trigonometric law is proposed. The method is applied to the visualisation of the in-plane vibrations by stroboscopic photographing of the structure in the state of equilibrium and in the state of extreme deflections. Finally, the method is modified for the analysis of circular structures producing digital angular and radial moiré fringes.

The procedure of numerical formation of moiré fringes can be applied in the process of the planning of experimental investigation enabling the selection of optimal spacing between the lines. Another useful application of the numerical method is the identification of the structural parameters when comparison between optical and simulated patterns can help to detect such physical values like the modulus of elasticity.

References

1. Timoshenko, S.P., Goodier, J.N., *Theory of Elasticity*, Nauka, Moscow, 1975.
2. Soifer, V.A., "Computer Processing of Images," *Herald of the Russian Academy of Sciences,* Vol. **71**(2), 2001, pp. 119–129.
3. Zienkiewicz, O.C., Morgan, K., *Finite Elements and Approximation*, Mir, Moscow, 1986.
4. Bathe, K.J., *Finite Element Procedures in Engineering Analysis*, Prentice-Hall, New Jersey, 1982.
5. Ramesh, K., and Pathak, P.M., "Role of Photoelasticity in Evolving Discretization Schemes for FE Analysis," *J. Experimental Techniques*, July/August, 1999, pp. 36–38.
6. Vest, C., *Holographic interferometry,* Mir, Moscow, 1982.
7. Post, D., Han, B.T., Ifju, P.G., "Moiré Methods for Engineering and Science—Moiré Interferometry and Shadow Moiré," *Photo—Mechanics Topics in Applied Physics,* **77**, 2000, pp. 151–196.
8. Han, B., Post, D., Ifju, P., "Moiré Interferometry for Engineering Mechanics: Current Practices and Future Developments," *Journal of Strain Analysis for Engineering Design,* Vol. **36**(1), 2001, pp. 101–117.